The Lowest Lying Singlet and Triplet States of the Halonitrenium Ions NX_2^+ and NHX^+ and a Comparison with the Carbon Analogues CX_2 and CHX (X=F, Cl, Br, I).# A Theoretical Study[1)]

Alberto GOBBI and Gernot FRENKING*
Fachbereich Chemie der Philipps-Universität Marburg, Hans-Meerwein-Strasse, D-35037 Marburg, Germany
(Received April 8, 1993)

The equilibrium geometries, energy differences, and vibrational frequencies for the energetically lowest lying $^1A_1$ and $^3B_1$ states of NH_2^+, NHX^+, and NX_2^+ (X=F, Cl, Br, I) are theoretically predicted using ab initio quantum mechanical methods at the MP4/6-311G(2df)//MP2/6-31G(d) level of theory. Effective core potentials are employed for bromine and iodine. The isoelectronic carbenes CH_2, CHX, and CX_2 are also calculated. The electronic structure of the molecules is investigated using the topological analysis of the electronic wave function.

Methylene has a ($^3B_1$) ground state, which is 9.0 kcal mol^{-1} lower in energy than the first excited ($^1A_1$) singlet state.[2)] The singlet–triplet gap of CH_2 has been the subject of numerous theoretical papers[3—6)] and two reviews of the theoretical studies are published.[7)] The early disagreement between the experimentally reported and theoretically predicted first excitation energy of methylene was finally resolved in favor of theory.[6)] Theory also played a role in the prediction of the electronic ground state of the halogen substituted methylenes CHX and CX_2 (X=F, Cl, Br, I).[8—13)] Difluoromethylene CF_2 has a ($^1A_1$) singlet ground state, which is 56.7 kcal mol^{-1} more stable than the ($^3B_1$) triplet state, in good agreement with theoretical predictions (55.6—57.5 kcal mol^{-1}).[8,11)] Only few experimental data are reported for the other halogen substituted methylenes. Upper bounds for the ($^3B_1$)←($^1A_1$) excitation energy are reported for CHF, CHCl, CHBr, and CHI.[15)] The halogen substituted methylenes CHX and CX_2 (X=F, Cl, Br, I) have been studied theoretically with exception of CHI.[8—13)] All investigated molecules CHX and CX_2 with X=halogen are predicted to have a ($^1A_1$) singlet ground state.[8—13)] The singlet–triplet gap is lower in CHX than in CX_2 for a given halogen atom X and it becomes smaller with the order F>Cl>Br>I. The stabilization of the singlet state by the halogen atoms has been attributed to the π-donor ability of the substituents.[16,17)] An alternative explanation is based upon the electronegativity of the subsituents X in CX_2, which yields a larger HOMO–LUMO gap when X becomes more electronegative.[10,11,18)]

The nitrenium ion NH_2^+ is isoelectronic to methylene. In contrast to the latter, however, NH_2^+ and its halogen substituted derivatives NHX^+ and NX_2^+ have received very little attention. Like CH_2, NH_2^+ has a ($^3B_1$) ground state which is 30.1 kcal mol^{-1} lower in energy than the ($^1A_1$) first excited state.[19)] This is in good agreement with theoretically predicted singlet–triplet gaps of 29.1—32.4 kcal mol^{-1} for NH_2^+.[20—24)] Thus, the ($^1A_1$)←($^3B_1$) excitation energy of NH_2^+ is clearly larger than for CH_2. The only halogen substituted nitrenium ions studied so far are NHF^+ and NF_2^+. The ($^1A_1$) ground state of NF_2^+ has theoretically been investigated by three different groups.[25—27)] The reaction of NF_2^+ with CH_4 was studied experimentally using ion cyclotron resonance techniques.[27)] Among other products, the formation of the radical cation $CH_3NFH^{+\bullet}$ was observed, which was explained by the presence of a triplet state of NF_2^+.[27)] The only theoretical study of the singlet–triplet gap of halogen substituted nitrenium ions is an early report for NHF^+ and NF_2^+, but on a rather low level of theory.[28)] There are no experimental or theoretical studies of other halogen subsituted nitrenium ions NHX^+ and NX_2^+ known to us.

In this paper we wish to report the results of the first systematic ab initio investigation of the molecules NHX^+ and NX_2^+ (X=F, Cl, Br, I). For comparison, we also studied NH_2^+ and the methylene analogues CH_2, CHX and CX_2 (X=H, F, Cl, Br, I). We calculated the geometries, energies and vibrational frequencies of the lowest lying $^3B_1$ and $^1A_1$ states, and we studied the electronic structure of the molecules using the topological analysis of the electron density distribution developed by Bader and coworkers.[29)] Relativistic effective core potentials[30)] (ECP) are used for Br and I, and all-electron basis sets are employed for the other atoms. The contribution of correlation energy is estimated using Møller–Plesset perturbation theory.[31)]

Theoretical Methods

The geometries for the lowest lying $^1A_1$ and $^3B_1$ electronic states of the investigated molecules have been optimized using Møller–Plesset perturbation theory[31)] terminated at second order (MP2) using the ECP by Wadt and Hay[30)] for bromine and iodine and the 6-31G(d) all electron basis set[32)] for the other atoms. The (3/3) minimal valence basis sets for Br and I are uncontracted and augmented by a set of d-type polarization functions[33)] with exponents ζ_d=0.428 (Br) and ζ_d=0.289 (I), i.e. the basis set is [21/21/1]. Unrestricted (UHF) wave functions[34)] are calculated for the

#This study is dedicated to the memory of Professor Hiroshi Kato.

triplet state and spin restricted (RHF) wave functions for the singlet states. All electrons are included in the correlation treatment. The vibrational frequencies and zero-point energies (ZPE) are calculated at the same level of theory. The ZPE corrections are scaled by 0.9.[35]

Improved total energies are predicted at the MP4 (SDTQ) level using the uncontracted ECP valence basis sets augmented by two sets of d functions[33] and one set of f functions[36] [111/111/11/1] for Br and I in conjunction with a 6-311G(2d,f) basis set[37] for the other atoms. The exponents for the polarization functions at Br and I are $\zeta_{d1}=0.214$ (Br); $\zeta_{d2}=0.856$ (Br); $\zeta_{f}=0.569$ (Br); $\zeta_{d1}=0.1445$ (I); $\zeta_{d2}=0.578$ (I); $\zeta_{f}=0.433$ (I).[33,36] The MP4 (SDTQ) calculations are carried out with the frozen-core approximation. Unless otherwise noted, energies are discussed at the MP4/6-311G(2df)//MP2/6-31G(d)+ZPE level of theory. All calculations were performed using the Gaussian 92 program series.[38] For the calculation of the electron density distribution $\rho(\boldsymbol{r})$, the gradient vector field $\nabla\rho(\boldsymbol{r})$, and its associated Laplacian $\nabla^2\rho(\boldsymbol{r})$ the programs PROAIM, SADDLE, GRID, and GRDVEC were used.[39]

Results and Discussion

Table 1 shows the theoretically predicted energy differences between the ($^1A_1$) singlet state and ($^3B_1$) triplet state for the carbenes and nitrenium ions in comparison with experimental data and previously calculated results. The total energies are shown in Table 2, the optimized geometries in Table 3.

The ($^1A_1$) singlet state of CH_2 is predicted 12.9 kcal mol^{-1} higher in energy than the ($^3B_1$) ground state, 2.9 kcal mol^{-1} higher than experimentally observed.[2] The error in the calculated value is mainly due to the one-configurational treatment of the singlet state. It has been shown that a much better agreement with experiment is obtained when at least a two-configuration (TCSCF) wave function is used as reference for ($^1A_1$) CH_2.[10,40] A multiconfigurational wave function appears not to be necessary for the halogen substituted methylenes. Table 1 shows that the calculated excitation energy from the ($^1A_1$) ground state to the ($^3B_1$) first excited state of CF_2 (57.6 kcal mol^{-1}) is in very good agreement with the experimental value (56.7 kcal mol^{-})[15] and with calculated results predicted at other high levels of theory. The agreement of the theoretical values calculated for other halogen substituted carbenes CHX and CX_2 with ab initio results obtained at a multiconfigurational level is also very good. In particular, we want to point out the very similar results calculated at the correlation consistent CI (CCCI) and dissociation consistent CI (DCCI) level of theory reported by Goddard and coworkers[8] for CF_2, CCl_2, CHF, CHCl, and our results. Also the TCSCF+CI results for CHF, CHCl, CHBr reported by Scuseria et al.[9] are not very different from our data (Table 1). Therefore, we think that the theoretically predicted singlet–triplet energy differences for the halogen substituted molecules reported in this study are quite reliable.

There are few experimental results for the singlet–triplet gap reported for CHX and CX_2 molecules (X= halogen). From the detailed analysis of the photoelectron spectrum of CHF it was suggested that the triplet excitation energy is 11.4±0.3, 14.7±0.2, or 8.1±0.4 kcal mol^{-1}, with the first value the most likely.[15] The theoretical results shown in Table 1 indicate that the experimental value 14.7±0.2 kcal mol^{-1} appears to be correct, but the value 11.4±0.2 kcal mol^{-1} cannot be ruled out. The triplet excitation energy of CHCl was reported by Murray et al.[15] to be (11.4±0.3)−n(2.5±0.2) kcal mol^{-1}. The theoretical results calculated by us and by others[8c,9] shown in Table 1 suggest that the correct value is either 3.9±0.9 or 6.4±0.7 kcal mol^{-1}.

A comparison with the theoretical results using density functional theory (DFT) is very interesting.[11] The singlet–triplet gap calculated at the DFT level is slightly too small for CF_2, but it is larger for CCl_2, CBr_2, and CI_2 than calculated here. Because our values for CCl_2 and CHBr agree very well with other high level ab initio calculations, we think that the excitation energies for CBr_2 and CI_2 predicted here are probably correct. This means that the singlet–triplet gap using the local density approximation (LDA) is slightly too large for CCl_2, CBr_2 and CI_2, and that the nonlocal exchange correction (NL) even worsens the results.[11]

Now we discuss the relative energies of the $^1A_1$ and $^3B_1$ states of the nitrenium ions. Table 1 shows that the calculated ($^1A_1$)←($^3B_1$) excitation energy for NH_2^+ (33.5 kcal mol^{-1}) is 3.4 kcal mol^{-1} higher than found by experiment (30.1 kcal mol^{-1}),[19] similar to the results calculated for CH_2. As for methylene, halogen substitution in NH_2^+ yields a ($^1A_1$) ground state for NHX^+ and NX_2^+ ions. While the singlet–triplet gap for NH_2^+ is clearly larger than for CH_2, the calculated excitation energies ($^3B_1$)←($^1A_1$) for the corresponding halogen substituted analogues CX_2 and NX_2^+ are nearly the same (Table 1). The theoretically predicted singlet–triplet gap for NF_2^+ is 57.3 kcal mol^{-1} (57.6 kcal mol^{-1} for CF_2), for NCl_2^+ it is 19.8 kcal mol^{-1} (20.5 kcal mol^{-1} for CCl_2, for NBr_2^+ it is 16.3 kcal mol^{-1} (16.5 kcal mol^{-1} for CBr_2), and for NI_2^+ it is 11.3 kcal mol^{-1} (11.2 kcal mol^{-1} for CI_2).

Slightly different singlet–triplet gaps are predicted for the mono halogen ions NHX^+ than for CHX. Table 1 shows that for NHF^+ a lower excitation energy (8.1 kcal mol^{-1}) is predicted than for CHF (14.3 kcal mol^{-1}), while the values for $NHCl^+$ (4.1 kcal mol^{-1}) and CHCl (4.8 kcal mol^{-1}) are very similar. The singlet–triplet gaps calculated for $NHBr^+$ (6.4 kcal mol^{-1}) and NHI^+ (7.5 kcal mol^{-1}) are larger than for CHBr (4.4 kcal mol^{-1}) and CHI (2.6 kcal mol^{-1}). $NHBr^+$ and NHI^+ are predicted to be exceptions from the rule that the ($^3B_1$)←($^1A_1$) excitation energy of molecules AHX and AX_2 decreases with decreasing electronegativity of the terminal atoms. There are no experimental results available for halogen substituted nitrenium ions to com-

Table 1. Theoretically Predicted and Experimentally Derived Energy Differences (kcal mol^{-1}) between the Lowest Lying $^1A_1$ and $^3B_1$ States
Negative Values Indicate That the $^3B_1$ State is the Ground State.

	HF/6-311G(2df)	MP2/6-311G(2df)	MP3/6-311G(2df)	MP4/6-311G(2df)	MP4/6-311G(2df) +ZPE	Exp.	Calcd[a] CCCl/DCCl	Calcd[b] TCSCF +Cl	Calcd[c] DFT LDA, LDA/NL	Calcd (other)
CH_2	−28.4	−16.5	−14.1	−13.4	−12.9	−8.998—−9.023[d]	−10.0, −9.0		−12.22, −7.20	−9.1[c]
CF_2	32.2	53.8	53.1	57.6	57.6	56.7[f], >50.[g]	57.1, 57.5		55.8, 55.6	
CCl_2	−5.2	17.2	15.6	20.2	20.5		25.9, 20.5		21.91, 23.75	
CBr_2	10.5	13.0	10.5	16.7	16.5				20.89, 22.41	7.7[b]
Cl_2	−18.2	7.0	3.1	11.5	11.2				15.73, 16.49	
CHF	−6.1	10.4	11.3	14.3	14.3	14.7; 11.4; 8.1[g]	14.5, 17.7	13.2		
CHCl	−15.7	1.5	2.0	4.8	4.8	<11.4[g]	9.3, 6.0	5.4		
CHBr	−17.0	0.7	1.0	4.3	4.4	<9.[g]		4.1		
CHI	−19.9	−1.4	−1.5	2.6	2.6	<9.[g]				
NH_2^+	−50.4	−36.6	−34.1	−32.9	−33.5	−30.1[i], −22.8 [i]				−33.2,[k] −29.7,[l] −45.[m]
NF_2^+	19.8	54.5	46.4	57.8	57.3					33.[m]
NCl_2^+	−15.3	19.4	11.5	20.1	19.8					
NBr_2^+	−23.3	16.0	5.3	17.1	16.3					
NI_2^+	−31.4	11.2	−2.2	12.0	11.3					
NHF^+	−19.8	4.6	1.9	8.7	8.1					−4.[m]
$NHCl^+$	−23.9	2.7	−1.0	4.6	4.1					
$NHBr^+$	−25.9	4.9	−0.5	7.0	6.4					
NHI^+	−29.1	6.4	−1.3	8.0	7.5					

a) Ref. 8. b) Ref. 9. c) Ref. 11. d) Ref. 2. e) Ref. 3. f) Ref. 14. g) Ref. 15. h) Ref. 10. i) Ref. 19. j) Ref. 44. k) Ref. 24. l) Ref. 21. m) Ref. 28.

Table 2. Calculated Total Energies (a.u.) for the $^1A_1$ State Using Geometries Opitimized at the MP2/6-31G(d) Level with ECP's for Br, I

	E_{tot} HF/6-311G(2df)	MP2/6-311G(2df)	MP3/6-311G(2df)	MP4/6-311G(2df)
CH_2	−38.88652	−39.01080	−39.03080	−39.03656
CF_2	−236.73872	−237.6448	−237.36378	−237.39969
CCl_2	−956.7892	−957.28990	−957.32444	−957.35563
CBr_2	−63.63899	−64.09896	−64.11728	−64.16148
CI_2	−60.07882	−60.50080	−60.51200	−60.56322
CHF	−137.80031	−138.17567	−138.18529	−138.20723
CHCl	−497.84069	−498.15400	−498.18223	−498.20034
CHBr	−51.26862	−51.55873	−51.57970	−51.60354
CHI	−49.48891	−49.75897	−49.77772	−49.80382
NH_2^+	−55.14547	−55.28956	−55.30987	−55.31632
NF_2^+	−252.81017	−253.49369	−253.48030	−253.53831
NCl_2^+	−972.99144	−973.55255	−973.57408	−973.62193
NBr_2^+	−79.87482	−80.38701	−80.39932	−80.46459
NI_2^+	−76.35887	−76.84834,	−76.83707	−76.91137
NHF^+	−153.97786	−154.39462	−154.39719	−154.43104
$NHCl^+$	−514.08780	−514.45196	−514.47095	−514.50002
$NHBr^+$	−67.53018	−67.88037	−67.88863	−67.92701
NHI^+	−65.77466	−66.1131	−66.11535	−66.16005

pare our theoretical excitation energies. In the light of the rather high ($^3B_1$)←($^1A_1$) excitation energy predicted for NF_2^+ it seems questionable, however, that a triplet state of NF_2^+ is indeed involved in the reaction of NF_2^+ with CH_4 yielding CH_4NF^+ as suggested by Fisher and McMahon.[27]

The only previous theoretical study on the singlet–triplet gap in substituted nitrenium ions was carried out at the SCF level with assumed N–F distances for NHF^+ and NF_2^+ by Harrison and Eakers.[28] It was predicted that NF_2^+ has a singlet ground state, 33 kcal mol^{-1} below the triplet state, and that NHF^+ has a triplet ground state 4 kcal mol^{-1} below the singlet.[28] This early study may not be very reliable due to the limited theoretical methods available at that time.

Table 3 shows the optimized geometries in com-

Table 3. Theoretically Predicted MP2/6-31G(d) and Experimentally Observed Geometries Interatomic Distances AB in Å, Angles ω in Degree.

	Calcd						Exptl					
	$^1A_1$			$^3B_1$			$^1A_1$			$^3B_1$		
	C/N-X	C/N-H	ω	C/N-X	C/N-H	ω	C/N-X	C/N-H	ω	C/N-X	C/N-H	ω
CH_2		1.109	102.1		1.078	131.5		1.11[a]	102.4[a]		1.0748[b]	133.84 [b]
CF_2	1.315		104.2	1.329		119.8	1.3035[c]		104.8[c]			
CCl_2	1.718		109.9	1.679		127.6	1.715[d]		109.2[d]			
CBr_2	1.893		111.0	1.840		129.9	1.74[e]		114.[e]	1.74[e]		150.[e]
CI_2	2.105		112.6	2.034		132.3						
CHF	1.320	1.121	101.9	1.329	1.086	121.2	1.305[f]	1.138[f]	104.1[f]			
CHCl	1.697	1.110	102.9	1.670	1.082	125.8	1.696[g]	1.130[g]	101.4[g]			
CHBr	1.862	1.110	101.9	1.827	1.082	126.5						
CHI	2.068	1.111	101.3	2.018	1.084	128.2						
NH_2^+		1.049	108.3		1.034	151.1						
NF_2^+	1.258		107.6	1.270		124.8						
NCl_2^+	1.608		117.3	1.582		137.0						
NBr_2^+	1.771		118.9	1.734		140.4						
NI_2^+	1.946		122.1	1.902		147.5						
NHF^+	1.246	1.055	104.2	1.245	1.055	125.4						
$NHCl^+$	1.549	1.045	109.1	1.524	1.037	134.1						
$NHBr^+$	1.704	1.042	107.9	1.669	1.033	134.5						
NHI^+	1.877	1.040	108.0	1.830	1.029	136.1						

a) Ref. 56. b) Ref. 46. c) Ref. 61d. d) Ref. 55. e) Ref. 41. f) Ref. 58. g) Ref. 59.

parison with experimental results for CHX and CX_2 molecules. There are no experimental geometries available for the nitrenium ions. We discuss the results for the carbenes first in order to estimate the accuracy of the predicted geometries. Generally, the agreement with experiment is quite good. The calculated bond lengths and bond angles for the $^3B_1$ and $^1A_1$ states of CH_2 and the $^1A_1$ state of CF_2, CCl_2, CHF, and CHCl are very similar to the experimental values. The C–F distances in CF_2 and CHF are calculated too long by 0.01—0.015 Å. In case of CBr_2, however, we think that the rather crude estimates of the bond lengths and angles taken from experiment[41] are probably not correct. The calculated geometries for the $^3B_1$ and $^1A_1$ states of CBr_2 agree well with previous theoretical results.[10,11] The calculated data shows the following trends for the methylenes: (i) the bond angle of the $^3B_1$ state is always larger than the angle of the corresponding $^1A_1$ state; (ii) the bond angle of the halogen substituted methylenes CHX and CX_2 increases with the order F<Cl<Br<I, except for the $^1A_1$ state of CHX which shows a rather constant bond angle; (iii) the C–X bond in the $^3B_1$ state is longer than in the $^1A_1$ state for CF_2, but shorter for the other CHX and CX_2 molecules.

The same trends (i)—(iii) calculated for the methylenes are also predicted for the nitrenium ions (Table 3). The bond angles are larger for the nitrenium ions than for the respective carbenes. This holds particularly for the ($^3B_1$) ground state of NH_2^+. Experimental studies by Okumura et al.[42] suggest that NH_2^+ is quasi-linear, but the estimated bending angle of 165° was probably too large because of the large amplitude of the bending vibration. The bond angle calculated here (151.1°) is in good agreement with previous theoretical studies by Peyerimhoff and Buenker,[21] who predict ω (NH_2^+)=149.6°, and by Jensen et al.[43] predicting ω (NH_2^+)=153.2°. The N–F bond length calculated for ($^1A_1$) NF_2^+ (1.258 Å) is nearly the same as predicted by Peterson et al.[25] using CASSCF methods (1.255 Å). The theoretically predicted geometries for NHX^+ and NX_2^+ ions shown in Table 3 may serve as a guideline for future experiments.

Table 4 shows the calculated harmonic vibrational frequencies and IR intensities for the methylenes and nitrenium ions in comparison with experimentally reported values. It is well known that the vibrational frequencies calculated using the harmonic approximation are usually too high by ca. 10% at this level of theory.[35] In particular, the stretching modes are predicted with wave numbers which are too high. The results in Table 4 show that the theoretical frequencies for the carbenes in the $^1A_1$ and $^3B_1$ state are always higher than experimentally observed. The *shift* of the vibrational frequencies upon substitution of the terminal atoms, however, is predicted quite reliably. The comparison of the theoretical frequencies with the available experimental results for the carbenes allows an estimate for the wave numbers of those fundamentals which have not been measured yet.

Experimental vibrational frequencies for NH_2^+ have been reported for the ($^3B_1$) ground state by Okamura et al.[42] and for the $^3B_1$ as well as several excited states

Table 4. Theoretically Predicted and Experimentally Observed Vibrational Frequencies (cm^{-1}) Calculated IR-Intensities ($km\,mol^{-1}$). Theoretical Values Calculated at MP2/6-31G(d) Using ECP's for Br, I.

	$^1A_1$								
	Calcd						Exptl		
	$\nu_{C/N-X}/\nu_s$	Int.	$\nu_{C/N-H}/\nu_{as}$	Int.	ν_{bend}	Int.	$\nu_{C/N-X}/\nu_s$	$\nu_{C/N-H}/\nu_{as}$	ν_{bend}
CH_2	3002	67.6	3086	111.1	1498	0.3	2806[a]	2865[a]	1353[b]
CF_2	1278	107.9	1175	361.2	665	3.7	1222–1234[c]	1102–1126[d]	663–670[e]
CCl_2	770	42.7	792	469.9	354	0.3	720–721[f]	748[g]	327[h]
CBr_2	618	23.4	665	413.3	206	0.6	595[i]		196[i]
CI_2	506	13.7	572	451.5	140	0.7			
CHF	1257	159.8	2879	186.1	1480	14.8	1180–1182[k,l]		1405[k]
CHCl	856	122.8	3001	90.2	1300	7.9	810–815[l,m]		1201[m]
CHBr	706	84.6	3011	80.4	1219	3.5	660[l]		
CHI	599	77.3	3010	65.2	1132	2.4	600[l]		
NH_2^+	3268	63.3	3380	196.2	1511	99.2	2900[n]		1350[n]
NF_2^+	1386	52.5	1361	389.8	725	8.3	1250[o]		
NCl_2^+	860	0.5	1010	516.4	408	0.0			
NBr_2^+	681	0.0	871	554.8	248	0.1			
NI_2^+	575	3.4	801	696.3	177	0.4			
NHF^+	1508	44.5	3223	71.7	1569	123.7			
$NHCl^+$	1152	4.3	3305	85.3	1367	75.3			
$NHBr^+$	969	0.4	3335	79.3	1283	65.6			
NHI^+	883	10.9	3355	62.9	1210	58.3			

	$^3B_1$								
	Calcd						Exptl		
	$\nu_{C/N-X}/\nu_s$	Int.	$\nu_{C/N-H}/\nu_{as}$	Int.	ν_{bend}	Int.	$\nu_{C/N-X}/\nu_s$	$\nu_{C/N-H}/\nu_{as}$	ν_{bend}
CH_2	3248	1.4	3469	0.5	1195	6.8	2992[p]	3213[rmp]	
CF_2	1171	52.1	1363	272.6	509	9.1			
CCl_2	723	6.6	1044	224.7	315	0.2			
CBr_2	546	1.3	897	168.5	194	0.0			
CI_2	431	0.0	802	140.6	136	0.2			
CHF	1302	85.8	3247	10.0	1165	35.6	1170[l]		1170[l]
CHCl	992	53.4	3306	8.6	1052	0.7	870[l]		
CHBr	763	28.3	3303	6.4	975	2.2			
CHI	659	16.1	3294	5.8	911	5.0			
NH_2^+	3328	49.5	3592	663.4	794	174.8		3359.9[q]	840[n]
NF_2^+	1194	20.3	1372	256.9	561	10.4			520[o]
NCl_2^+	718	0.0	1048	526.2	353	0.7			
NBr_2^+	506	0.2	885	602.5	220	1.3			
NI_2^+	357	2.4	786	811.8	148	2.9			
NHF^+	1505	112.7	3202	337.2	1120	127.9			
$NHCl^+$	1145	82.9	3414	347.0	929	202.4			
$NHBr^+$	937	74.7	3456	348.2	812	265.0			
NHI^+	798	101.8	3508	343.1	674	358.5			

a) Ref. 60. b) Ref. 56. c) Ref. 61. d) Refs. 61f and 61g. e) Refs. 62, 61a, 61d, and 61f. f) Ref. 63. g) Refs. 63 and 64. h) Ref. 65. i) Ref. 66. j) Ref. 67. k) Ref. 68. l) Ref. 15. m) Ref. 69. n) Ref. 44. o) Ref. 45. p) Ref. 70. q) Ref. 42.

of NH_2^+ by Dunlavy et al.[44] Table 4 shows that the (unscaled) theoretical vibrations for the fundamentals of NH_2^+ show a similar agreement with experiment than for CH_2. The only experimentally reported vibrational frequencies for halonitrenium ions are available for NF_2^+. The calculated frequencies for the symmetric and asymmetric NF stretching mode are higher than in ($^1A_1$) CF_2 (Table 4). This is in agreement with the measured value of 1250 cm^{-1} for the symmetric stretching mode of ($^1A_1$) NF_2^+ as reported by Cornford et al.,[45] which is higher than the observed[46] symmetric stretching mode (1222—1234 cm^{-1}) for CH_2. The same

authors also reported vibrational intervals for the $^3B_1$ state of NF_2^+ at 520 cm^{-1}, which they assign to the N–F stretching mode in this state assuming a significantly weaker N–F bond than in the ground state.[45] Our calculations agree that the N–F bond in the $^3B_1$ state of NF_2^+ is longer than in the $^1A_1$ state. However, the theoretically predicted frequency for the symmetric stretching mode for ($^3B_1$) NF_1^+ is 1194 cm^{-1}, which is too high to support the assignment of the observed vibrational intervals at 520 cm^{-1} to the stretching vibration (Table 4). The observed value of 520 cm^{-1} is in much better agreement with the calculated bending mode at 561 cm^{-1}.

Why is the ($^1A_1$)←($^3B_1$) excitation energy of NH_2^+ significantly higher than for CH_2, while the singlet–triplet gap of the halogen substituted nitrenium ions is nearly the same as for the respective methylene? This surprising result can be explained using frontier orbital arguments[47] and Mulliken-Walsh type diagrams.[48] Figure 1 shows a schematic representation of the valence orbitals of AH_2 molecules and the change of the energy levels upon bending.

For linear AH_2 molecules with six valence electrons such as CH_2 and NH_2^+ the $1\sigma_g$ and $1\sigma_u$ valence MOs are doubly occupied in the ground state and the degenerate π_u MO is occupied by two electrons with the same spin, yielding a $^3\Sigma_g^-$ state. Upon bending, the π_u MO is split into the $1b_1$ (π) MO and the $2a_1$ MO (Fig. 1).

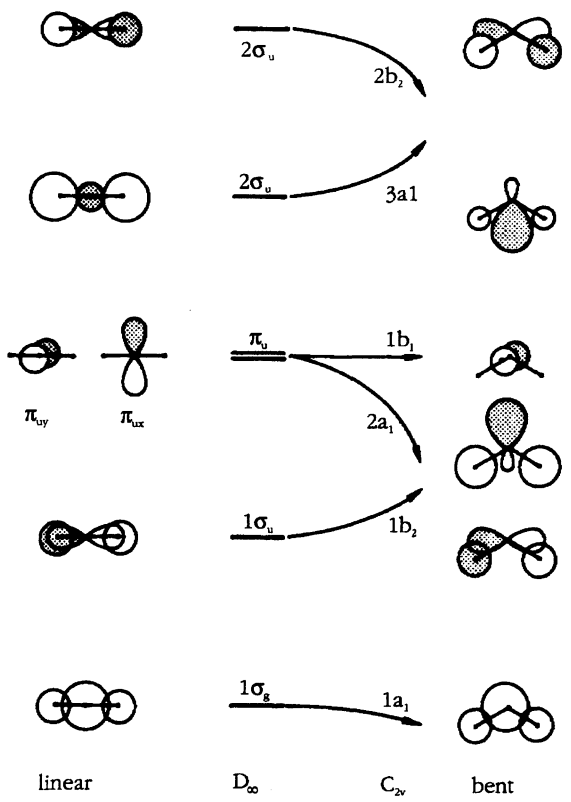

Fig. 1. Schematic representation of the most important valence orbitals of AH_2 molecules.

The energy level of the $1b_1$ MO does not change upon bending, but the $2a_1$ orbital becomes lower in energy when the bond angle becomes smaller. If the energy gap between the $1b_1$ and $2a_1$ MO is large enough to compensate for the exchange term, the $^1A_1$ state with a doubly occupied $2a_1$ MO becomes the ground state. It follows that the $^1A_1$ states of CH_2 and NH_2^+ should have smaller bond angles than the $^3B_1$ states. This is indeed the case (Table 1). The energy lowering of the $2a_1$ orbital of AH_2 is due to the mixing of the $2a_1$ and $3a_1$ MOs, which raises the energy of the latter orbital. The mixing becomes more important the higher the energy of the $2a_1$ and the lower the energy of the $3a_1$ MO. Because nitrogen is more electronegative than carbon, the $2a_1$ MO is lower lying in NH_2^+ than in CH_2, and the $2a_1$–$3a_1$ mixing therefore weaker in the former than in the latter molecule. As a consequence, the energy gap between the $2a_1$ and $1b_1$ MOs is smaller and the singlet–triplet gap and the bonding angles are larger in NH_2^+ than CH_2 (Tables 1 and 2). In particular, the bonding angle in ($^3B_1$) NH_2^+ (151.1°) is significantly larger than in ($^3B_1$) CH_2 (131.5°).

What about the halogen substituted systems CX_2 and NX_2^+? Figure 2 shows schematically the most important valence orbitals for the system AB_2. In the 18 valence electron systems CX_2 and NX_2^+, the degenerate $2\pi_u$ orbital is occupied by two electrons. Upon bending, the $2\pi_u$ MO splits into the $4a_1$ and $2b_1$ MOs (Fig. 2). Unlike the $1\pi_u$ orbital of AH_2, however, *both* components of the $2\pi_u$ MO of AB_2, i.e. the $4a_1$ and $2b_1$ MOs, are stabilized upon bending, though to a different extent. The $2b_1$ orbital becomes slightly lower in energy because of the in-phase π-type overlap of the terminal p orbitals. The $4a_1$ orbital is lowered due to the mixing with the $5a_1$ orbital (Fig. 2). Since the $2b_1$ orbital of CF_2 and NF_2^+ is stabilized upon bending, the $^3B_1$ states of these molecules with a singly occupied $2b_1$ MO have significantly smaller angles (119.8° for CH_2, 124.8° for NF_2^+) than the $^3B_1$ states of CH_2 and NH_2^+ (131.5°

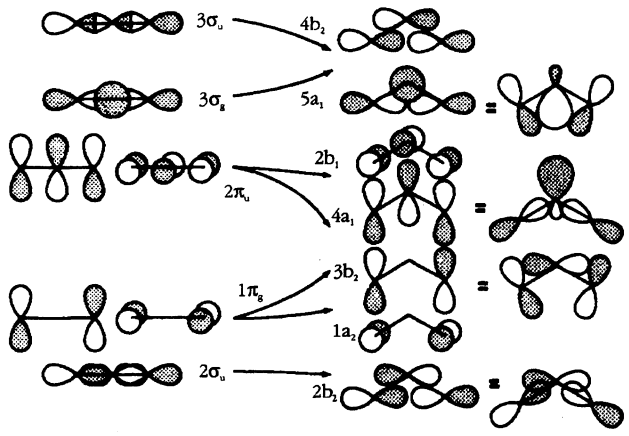

Fig. 2. Schematic representation of the most important valence orbitals of AB_2 molecules.

for CH_2, 151.1° for NF_2^+). The mixing of the $4a_1$ and $5a_1$ orbitals in NX_2^+ is weaker than in CX_2, similar to the $2a_1$–$3a_1$ orbital mixing in CH_2 and NH_2^+. However, since the $2b_1$ orbital in CF_2 and NF_2^+ is also lowered upon bending, the $(^3B_1)\leftarrow(^1A_1)$ excitation energy is less influenced by the different electronegativity of the central atom. Another difference between the AH_2 and AB_2 systems is, that the $2\pi_u$ MO in linear AB_2 has large coefficients at the terminal atoms, whereas the π_u MO of AH_2 has not (Figs. 1 and 2). The $4a_1$–$5a_1$ mixing in CF_2 and NF_2^+ involves mainly coefficients of the same atom type, i.e. the terminal fluorine atoms, whereas the $2a_1$–$3a_1$ mixing in CH_2 and N_2^+ is dominated by the coefficient of the central atom, which is different in the two molecules. Thus, the differences between the $^1A_1$ and $^3B_1$ states of CF_2 and NF_2^+ are much smaller than for CH_2 and NH_2^+. Table 1 shows that this holds true for all molecules CX_2 compared with NX_2^+.

We investigated the electronic structure of the carbenes and nitrenium ions using the topological analysis of the electronic wave functions developed by Bader and coworkers.[29] This method has been found in our previous theoretical studies on inorganic molecules[1] to give valuable information about the bonding and charge distribution in these molecules. A very detailed topological analysis of the electronic structures of carbenes including CH_2 and CF_2 in the $^1A_1$ and $^3B_1$ states has already been presented by MacDougall and Bader[49a] and by Gatti et al.[49b] Because other theoretical studies of halogen substituted carbenes[8—11] focussed mainly on the singlet–triplet gap and spectroscopic properties of the molecules without analyzing the wave function, we also discuss these molecules in detail.

The contour line diagrams of the Laplacian distribution $\nabla^2\rho(\boldsymbol{r})$ for the investigated molecules in the molecular plane are shown in Figs. 3 and 4. The results of the topological analysis of the wave functions are listed in Table 5. The calculated atomic partial charges obtained by numerical integration of the electron density in the atomic basins separated by the zero-flux surfaces are shown in Table 6.

The Laplacian distribution exhibited in Figs. 3 and 4 shows regions of electon depletion ($\nabla^2\rho(\boldsymbol{r})>0$, dashed lines) and electron concentration ($\nabla^2\rho(\boldsymbol{r})<0$, solid lines). The solid lines connecting the atomic nuclei are the bond paths.[29] The solid lines separating the nuclei indicate the zero-flux surfaces in the molecular plane. The points where the solid lines are crossing between the atoms are the bond critical points $\boldsymbol{r}_b$.[29] The position of $\boldsymbol{r}_b$ relative to the "non-polar midpoint" of a bond A–B may be used to define the effective electronegativity of the bonded atoms.[1] If A and B are identical, the midpoint is simply the half of the calculated interatomic distance. If A and B are different, the sum of the atomic radii α_A and α_B, corrected by the actual interatomic distance r_{AB}, may be used to define the "non-polar" midpoint of the A–B bond. If for the carbene bonds C–X the latter is given by its distance to the carbon atom m_C, we defined the nonpolar midpoint m_C:

$$m_C = \alpha_C \times r_{CX} \times (\alpha_C + \alpha_X)^{-1},$$

m_C=distance of the "non-polar" midpoint from atom C,
a_C=atomic radius of C in C–C single bond,
a_X=atomic radius of X in X–X single bond,
r_{CX}=calculated interatomic distance C–X.

For the nitrenium ions NHX^+ and NX_2^+ the corresponding equation holds with N for C. The atomic radii for the atoms were taken from the literature.[50]

The shift $\Delta\boldsymbol{r}_b$ from the "non-polar" midpoint of a bond A–B can then be taken as a measure for the effective electronegativity of the atoms.[1] Alternatively, the calculated partial charges of the atoms A and B may be used to define the relative electronegativity as suggested by Bader.[51] However, the integration involves all electrons of an atom, not only the electronic charge in the bond A–B. The partial charges in CO and CF calculated by Bader[51] would suggest that oxygen is more electronegative than fluorine, because the carbon atom carries a larger positive charge in the former molecule than in the latter. Since fluorine is definitely more electronegative than oxygen, the use of atomic charges as a measure of electonegativity is not very useful.

The shift in the bond critical point $\Delta\boldsymbol{r}_b$ shown in Table 5 for the carbenes is given by the distance between $\boldsymbol{r}_b$ and m_C for the C–X (C–H) bond, with negative (positive) values indicating that $\boldsymbol{r}_b$ is shifted towards the carbon (X) atom. A shift of the bond critical point $\boldsymbol{r}_b$ towards the carbon end of the C–X bond means that a larger area of the bond is attributed to the (more electonegative) atom X. Table 5 shows that the C–H, C–F, and C–Cl bonds in the $^1A_1$ and $^3B_1$ states of CH_2, CHX, and CX_2 have negative values for $\Delta\boldsymbol{r}_b$. This means that F, Cl, and H are more electronegative in the corresponding C–X bonds than carbon. The higher electronegativity of hydrogen in CH_2 does not mean that the partial charge at carbon is positive. Table 6 shows that the integration of the atomic space gives a slightly positive charge (+ 0.028) at hydrogen in the $^1A_1$ state and an even larger positive charge (+ 0.115) in the $^3B_1$ state. The fluorine and chlorine atoms carry a negative partial charge in the corresponding carbenes, as expected. The calculated charge distribution for CH_2 and CF_2 is very similar to the results given by Bader and coworkers[49]. Generally, the carbon atom in the methylenes is more positively charged in the $^1A_1$ state than in the $^3B_1$ state. A very interesting result of the topological analysis of the wave function is that the calculated charge distribution for the bromine substituted methylenes show a polarity C($\delta-$)–Br($\delta+$) for the C–Br bond (Table 6). Also the shift of the bond critical point $\Delta\boldsymbol{r}_b$ shows a lower electronegativity for bromine than for carbon (Table 5). The standard value for the

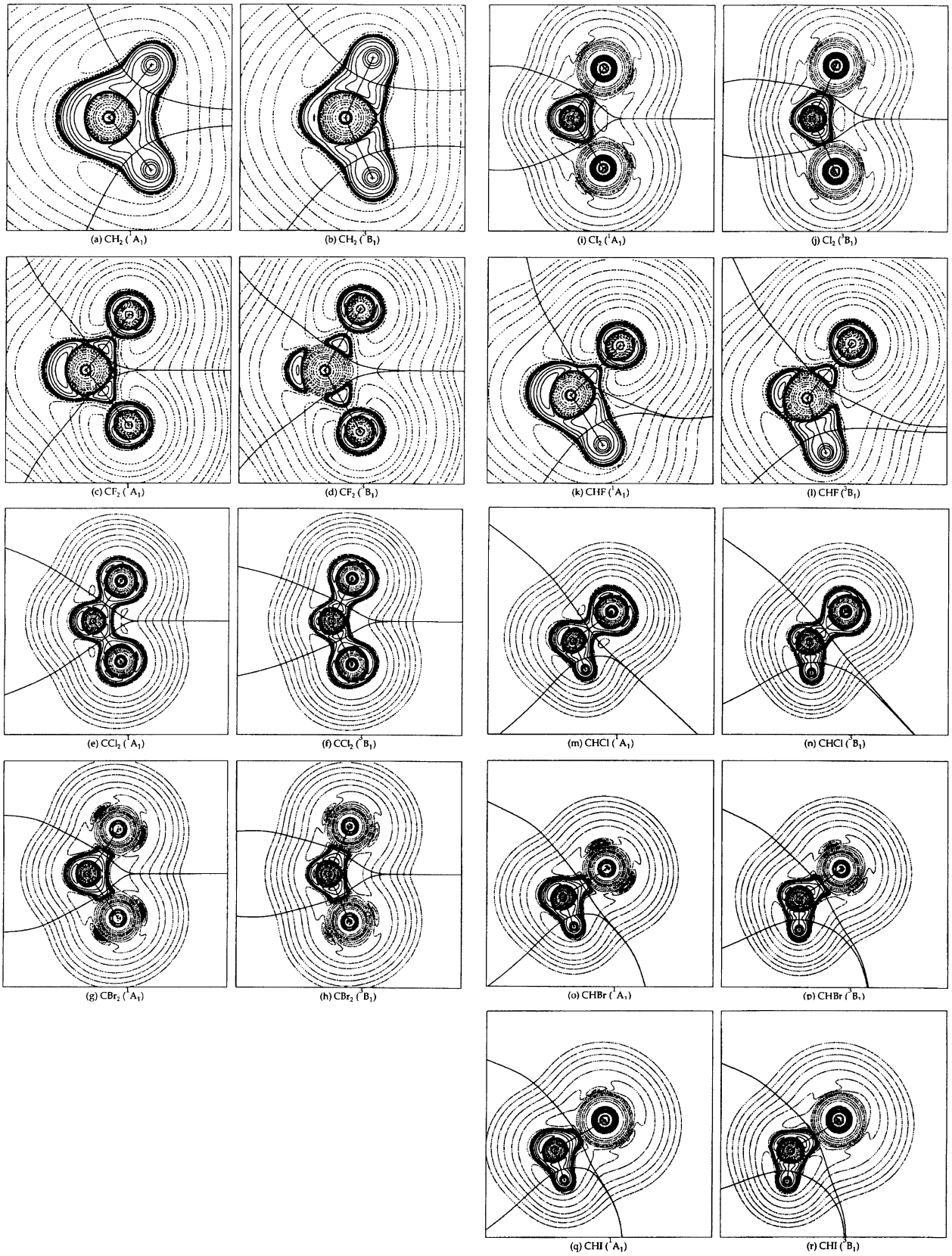

Fig. 3. Contour line diagrams of the Laplacian distribution $\nabla^2\rho(\boldsymbol{r})$ of the methylenes in the $^1A_1$ and $^3B_1$ states calculated at MP2/6-31G(d). Dashed lines indicate charge depletion ($\nabla^2\rho(\boldsymbol{r})>0$), solid lines indicate charge concentration ($\nabla^2\rho(\boldsymbol{r})<0$). The solid lines connecting the atomic nuclei are the bond paths, the solid lines separating the atomic nuclei indicate the zero-flux surfaces in the molecular plane.

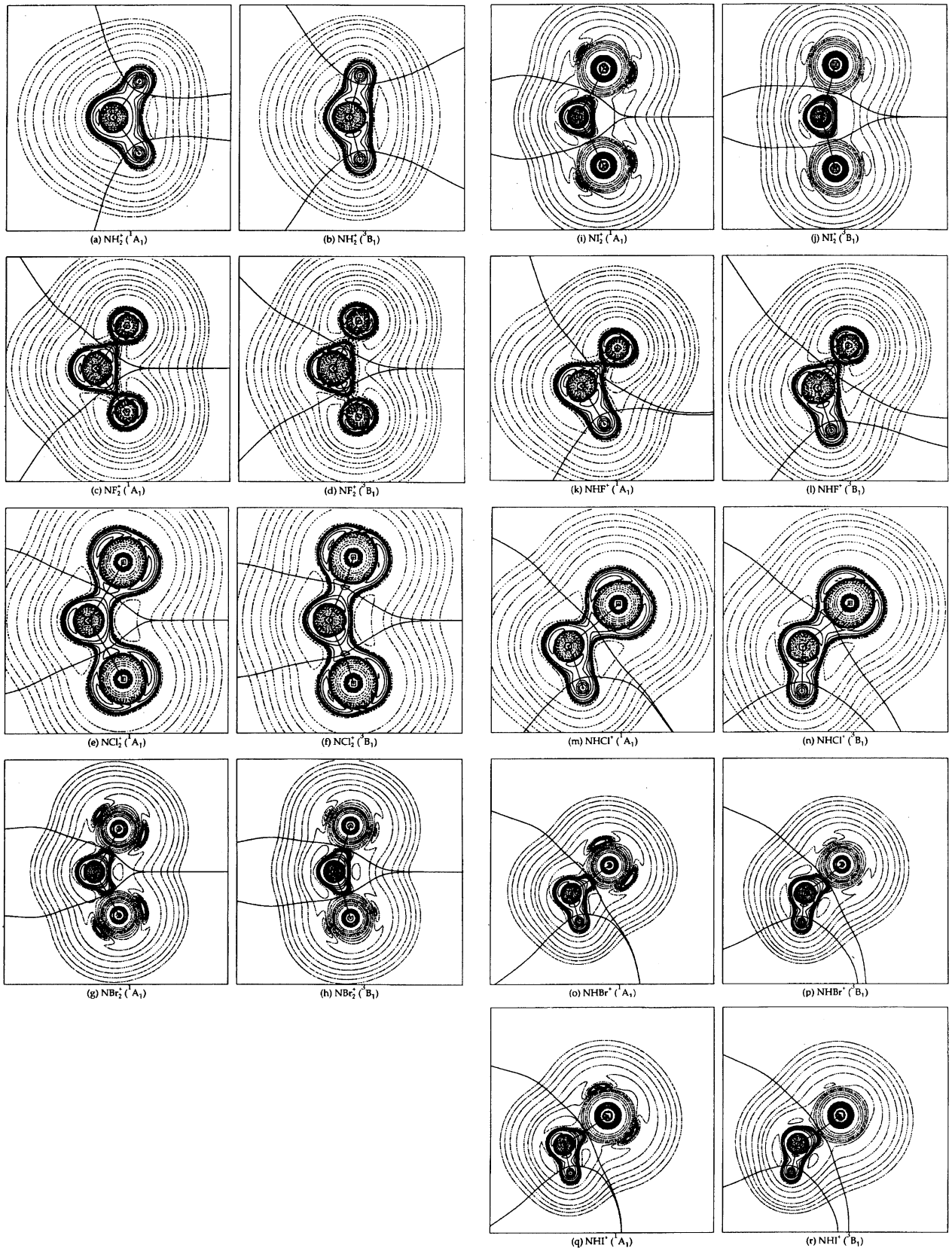

Fig. 4. Contour line diagrams of the Laplacian distribution $\nabla^2\rho(\boldsymbol{r})$ of the nitrenium ions in the $^1A_1$ and $^3B_1$ states calculated at MP2/6-31G(d). For details see Fig. 3.

Table 5. Results of the Topological Analysis at MP2/6-31G(d) Using ECP's for Br and I
Charge Density at the Bond Critical Point ρ_b(e/Å^3); Energy Density at the Bond Critical Point H_b (Hartree/Å^3); Location of the Bond Critical Point r_{bl} for the Bond A–B Given by A-r_b/A–B; Shift of the Bond Critical Point Relative to the "Non-Polar-Midpoint" as Defined in the Text Δr_b(Å); Ellipticity at the Bond Critical Point Parallel ε_b|| and Perpendicular $\varepsilon_b\perp$ to the Molecular Plane.

($^1A_1$)

	C/N-X					C/N-H				
	ρ_b	H_b	r_b	Δr_b	ε_b	ρ_b	H_b	r_b	Δr_b	ε_b
CH_2						1.836	−1.856	0.649	−0.079	0.133||
CF_2	1.849	−2.666	0.322	−0.294	0.346||					
CCl_2	1.424	−1.113	0.427	−0.017	0.019||					
CBr_2	1.080	−0.695	0.460	0.108	0.028||					
CI_2	0.803	−0.418	0.475	0.227	0.050⊥					
CHF	1.748	−2.402	0.321	−0.298	1.288||	1.856	−1.863	0.656	−0.076	0.038||
CHCl	1.451	−1.221	0.413	−0.041	0.124||	1.869	−1.923	0.657	−0.070	0.061||
CHBr	1.134	−0.769	0.451	0.090	0.021||	1.869	−1.917	6.659	−0.067	0.063||
CHI	0.857	−0.486	0.472	0.218	0.031⊥	1.849	−1.890	0.659	−0.067	0.069||
NH_2^+						2.072	−2.942	0.788	0.092	0.043||
NF_2^+	2.855	−3.928	0.419	−0.130	0.047⊥					
NCl_2^+	1.795	−1.795	0.506	0.147	0.095⊥					
NBr_2^+	1.275	−0.925	0.510	0.229	0.101⊥					
NI_2^+	0.958	−0.526	0.498	0.297	0.093⊥					
NHF^+	2.821	−4.272	0.398	−0.155	0.219||	2.112	−3.016	0.785	0.089	0.002||
$NHCl^+$	2.045	−2.315	0.506	0.142	0.117⊥	2.099	−2.956	0.776	0.079	0.010||
$NHBr^+$	1.478	−1.235	0.507	0.216	0.118⊥	2.105	−2.949	0.771	0.074	0.009||
NHI^+	1.113	−0.709	0.494	0.280	0.110⊥	2.099	−2.922	0.765	0.068	0.006||

($^3B_1$)

	C/N-X					C/N-H				
	ρ_b	H_b	r_b	Δr_b	ε_b	ρ_b	H_b	r_b	Δr_b	ε_b
CH_2						1.856	−1.964	0.653	−0.072	0.033⊥
CF_2	1.775	−2.510	0.324	−0.295	0.931⊥					
CCl_2	1.498	−1.221	0.431	−0.010	0.104⊥					
CBr_2	1.147	−0.790	0.476	0.133	0.066⊥					
CI_2	0.864	−0.486	0.488	0.246	0.045⊥					
CHF	1.721	−2.375	0.323	−0.297	0.324⊥	1.842	−1.944	0.659	−0.066	0.082⊥
CHCl	1.518	−1.289	0.421	−0.027	0.082⊥	1.842	−1.944	0.660	−0.064	0.052⊥
CHBr	1.188	−0.837	0.471	0.124	0.058⊥	1.842	−1.944	0.661	−0.064	0.050⊥
CHI	0.898	−0.526	0.488	0.245	0.045⊥	1.836	−1.930	0.660	−0.064	0.041⊥
NH_2^+						1.964	−2.747	0.797	0.101	0.004⊥
NF_2^+	2.713	−3.408	0.432	−0.115	0.151⊥					
NCl_2^+	1.768	−2.065	0.549	0.213	0.038⊥					
NBr_2^+	1.262	−0.898	0.523	0.248	0.024⊥					
NI_2^+	0.945	−0.452	0.503	0.300	0.018⊥					
NHF^+	2.841	−4.103	0.409	−0.141	0.083⊥	1.829	−2.531	0.797	0.103	0.021⊥
$NHCl^+$	2.031	−3.010	0.591	0.270	0.070⊥	1.930	−2.659	0.790	0.093	0.010⊥
$NHBr^+$	1.491	−1.242	0.523	0.237	0.034⊥	1.964	−2.706	0.786	0.089	0.010⊥
NHI^+	1.134	−0.634	0.501	0.287	0.032⊥	1.991	−2.740	0.781	0.083	0.005⊥

electronegativity of bromine suggested by Pauling[52] is higher (2.8) than for carbon (2.5), but it is known that the electronegativity is strongly influenced by the hybridization.

Visual inspection of the contour line diagrams exhibited in Fig. 3 shows charateristic differences among the methylenes. The C–H and C–Cl bonds are characterized by a continuous area of electron concentration, while the C–F bonds in CHF and CF_2 show that the electron distribution of the fluorine atoms is much less distorted than that of the carbon atom. Electronic charge at Br and I is largely depleted, which agrees with the calculated positive partial charges.

Further details about the bonding in the carbenes is given by the calculated ellipticity ϵ_b and the energy density at the bond critical point H_b (Table 5). The latter

Table 6. Calculated Partial Charges at MP2/6-31G(d)

	($^1A_1$)			($^3B_1$)		
	C/N	X	H	C/N	X	H
CH_2	−0.056		0.028	−0.230		0.115
CF_2	1.364	−0.682		1.258	−0.629	
CCl_2	0.242	−0.121		0.170	−0.085	
CBr_2	−0.030	0.015		−0.196	0.098	
Cl_2	−0.368	0.184		−0.596	0.298	
CHF	0.635	−0.653	0.018	0.510	−0.656	0.146
CHCl	0.097	−0.152	0.055	−0.015	−0.138	0.153
CHBr	−0.057	−0.010	0.067	−0.207	0.053	0.154
CHI	−0.248	0.177	0.071	−0.423	0.272	0.151
NH_2^+	−0.138		0.569	−0.284		0.642
NF_2^+	1.164	−0.082		1.096	−0.048	
NCl_2^+	−0.204	0.602		−0.378	0.689	
NBr_2^+	−0.470	0.735		−0.572	0.786	
NI_2^+	−0.864	0.932		−0.950	0.975	
NHF^+	0.520	−0.067	0.547	0.449	−0.104	0.655
$NHCl^+$	−0.327	0.815	0.512	−0.561	0.946	0.615
$NHBr^+$	−0.504	1.010	0.494	−0.608	1.013	0.595
NHI^+	−0.749	1.278	0.471	−0.867	1.297	0.570

property has been shown to correlate with the covalency of the corresponding bond, with negative values indicating a covalent bond, while a value of $H_b \approx 0$ suggest closed-shell interaction typical for ionic bonds or van der Waals interactions.[53] The calculated H_b values for the C–H and C–X bonds indicate a covalent character for all bonds. The covalency of the C–X bond decreases with the order F>Cl>Br>I. The covalency is slightly higher in the $^3B_1$ state than in the corresponding $^1A_1$ state, with exception of CF_2 (Table 5).

The final property listed in Table 5 is the bond ellipticity ϵ_b defined as $\epsilon_b=(\lambda_1/\lambda_2-1)$ where λ_1 and λ_2 are the magnitudes of the two negative curvatures of ρ at the bond critical point r_b with $|\lambda_1|>|\lambda_2|$.[54] When these two curvatures are not equal, the charge density of the covalent bond is accumulated in the plane containing the curvatures corresponding to λ_2. For example, the charge density of the C–C bond in ethylene is accumulated in the plane perpendicular to the molecular plane corresponding to the π bond. Table 5 shows that the charge of the C–H and C–X bonds of the $^3B_1$ state of the methylenes is always accumulated in the plane perpendicular ($\perp$) to the molecular plane. A large ϵ_b ($\perp$) value is calculated only for the C–F bonds in CF_2 and CHF. This indicates a strong π contribution to the C–F bond in these two molecules, particularly for CF_2. The ϵ_b values for the other C–X bonds are significantly smaller, i.e. the π contribution is weaker. Large ϵ_b values are also calculated for the $^1A_1$ ground state of CF_2 and CHF. However, the charge of the C–F bonds is accumulated in the molecular plane and not in the perpendicular plane as in the $^3B_1$ state (Table 5). The ϵ_b ($\parallel$) value of the C–F bond is much larger in CHF than in CF_2. The other C–X bonds show clearly smaller ϵ_b values.

The difference in the ellipticity of the C–F bonds in the $^1A_1$ and $^3B_1$ state of CF_2 is demonstrated by the contour line diagrams of the Laplacian in the plane perpendicular to the C–F bond containing the bond critical point r_b (Fig. 5). In the $^3B_1$ state, the C–F bond shows charge accumulation typical for a π bond perpendicular to the molecular plane (Fig. 5a). This explains the large value of ϵ_b ($\perp$)=0.931 (Table 5). In the $^1A_1$ state the C–F bond has nearly axial symmetry, the accumulation of electronic charge is higher in the molecular plane and higher on the "inside" of the molecule (Fig. 5b).

Now we discuss the results of the topological analysis for the nitrenium ions. The results of the topological analysis listed in Table 5 show that only for the N–F bonds the shift of the bond critical point Δr_b is calculated with a negative value, i.e. the other atoms are less electronegative than nitrogen. The numerical values show the same trend as for the methylenes. The nitrogen atoms carry a negative partial charge in all cations, with exception of the NHF^+ and NF_2^+ ions (Table 6). The N–X bonds of the nitrenium ions are more covalent than the corresponding C–X bonds in the carbenes, as revealed by the more negative H_b values (Table 5). The ellipticity of the N–F bonds in NHF^+ and NF_2^+ in the $^1A_1$ and $^3B_1$ state is lower than the C–F bonds in the corresponding methylenes. The halonitrenium ions in their $^3B_1$ state have N–H and N–X bonds with a small ellipticity ϵ_b perpendicular to the molecular plane. For the $^1A_1$ ground state of the halonitrenium ions a nearly constant value of ϵ_b ($\perp$)$\approx$0.1 is calculated for the C–X bonds, with exception of the C–F bonds.

Summary

The electronic ground state of the nitrenium cation NH_2^+ is theoretically predicted to have $^3B_1$ symme-

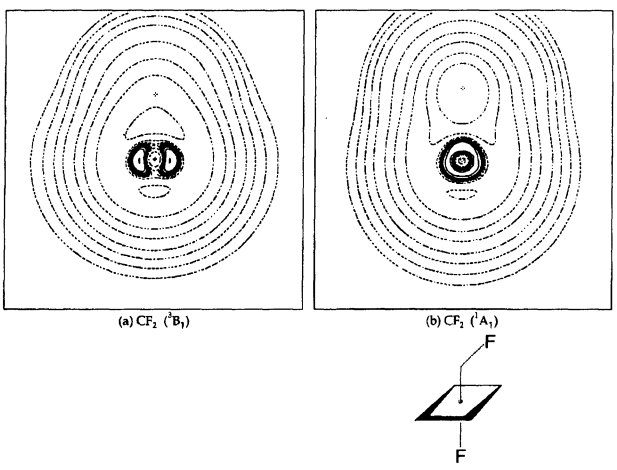

Fig. 5. Contour line diagrams of the Laplacian distribution $\nabla^2\rho(r)$ of CF_2 in the plane orthogonal to the C–F bond containing the bond critical point r_b; (a) $^3B_1$ state; (b) $^1A_1$ state.

try. The ($^1A_1$) first excited state is calculated to be 33.5 kcal mol^{-1} higher in energy than the ground state, which is in reasonable agreement with the experimental value of 30.1 kcal mol^{-1}. The halogen substituted analogues NHX^+ and NX_2^+ (X=F, Cl, Br, I) have a $^1A_1$ ground state. The singlet triplet gap is calculated as 57.3 kcal mol^{-1} for NF_2^+, 19.8 kcal mol^{-1} for NCl_2^+, 16.3 kcal mol^{-1} for NBr_2^+ and 11.3 kcal mol^{-1} for NI_2^+. The ($^3B_1$)←($^1A_1$) excitation energy for the monohalogen species NHX^+ is lower, 8.1 kcal mol^{-1} for NHF^+, 4.1 kcal mol^{-1} for $NHCl^+$, 6.4 kcal mol^{-1} for $NHBr^+$ and 7.5 kcal mol^{-1} for NHI^+. The calculated singlet triplet gap for the isoelectronic methylenes CH_2, CHX, and CX_2 is in good agreement with experimental results. The ($^3B_1$)←($^1A_1$) of NX_2^+ is predicted to be nearly the same as for the corresponding methylenes. The theoretically predicted geometries for the carbenes are also in good agreement with experimental data. The calculated vibrational frequencies suggest a reassignment of the vibrational progression observed for ($^3B_1$) NF_2^+ at 520 cm^{-1}. The topological analysis of the electronic wave function shows that the nitrenium ions have more covalent bonds than the corresponding carbenes. A strong π contribution is analyzed only for the C–F bonds in CF_2 and CHF.

We thank Professor K. Dehnicke for initiating this study. This work has been supported by the Fonds der Chemischen Industrie and the Deutsche Forschungsgemeinschaft. Additional support was provided by the HRZ Marburg, HLRZ Jülich, HHLR Darmstadt, and the computer companies Silicon Graphics and Convex.

References

1) Theoretical Studies of Inorganic Compound. Part III. Part I:M. Otto, S. D. Lotz and G. Frenking, *Inorg. Chem.*, **31**, 3647 (1992); Part II:A. Veldkamp and G. Frenking, *Chem. Ber.*, in press.

2) A. R. W. McKellar, P. R. Bunker, T. J. Sears, K. M. Evenson, R. J. Saykally, and S. R. Langhoff, *J. Chem. Phys.*, **79**, 5251 (1983); D. G. Leopold, K. K. Murray, and W. C. Lineberger, *J. Chem. Phys.*, **81**, 1048 (1984); D. G. Leopold, K. K. Murray, A. E. S. Miller, and W. C. Lineberger, *J. Chem. Phys.*, **83**, 4849 (1985); P. R. Buenker and T. J. Sears, *J. Chem. Phys.*, **83**, 4866 (1985).

3) E. A. Carter and W. A. Goddard, III, *J. Chem. Phys.*, **86**, 862 (1987).

4) C. W. Bauschlicher, S. R. Langhoff, and P. R. Taylor, *J. Chem. Phys.*, **87**, 387 (1987).

5) C. L. Jansen and H. F. Schaefer, III, *Theor. Chim. Acta*, **79**, 1 (1991).

6) R. B. Murphy and R. P. Messmer, *Chem. Phys. Lett.*, **183**, 443 (1991).

7) H. F. Schaefer, III, *Science*, **231**, 1100 (1986); P. R. Bunker, in "Comparison of ab initio Quantum Chemistry with Experiment," ed by R. J. Bartlett, Reidel, Dordrecht (1985).

8) E. A. Carter and W. A. Goddard, III, *J. Phys. Chem.*, **91**, 4651 (1987); E. A. Carter and W. A. Goddard, III, *J. Chem. Phys.*, **88**, 1752 (1988); S. K. Shin, W. A. Goddard, III, and J. L. Beauchamp, *J. Phys. Chem.*, **94**, 6963 (1990); S. K. Shin, W. A. Goddard, III, and J. L. Beauchamp, *J. Chem. Phys.*, **93**, 4986 (1990).

9) G. E. Scuseria, M. Duran, R. G. A. R. MacLagan, and H. F. Schaefer, III, *J. Am. Chem. Soc.*, **108**, 3248 (1986).

10) C. W. Bauschlicher, *J. Am. Chem. Soc.*, **102**, 5492 (1980); C. W. Bauschlicher, H. F. Schaefer, III, and P. S. Bagus, *J. Am. Chem. Soc.*, **99**, 7106 (1977).

11) G. L. Gutsev and T. Ziegler, *J. Phys. Chem.*, **95**, 7220 (1991).

12) D. A. Dixon, *J. Phys. Chem.*, **90**, 54 (1986).

13) B. T. Luke, J. A. Pople, M. -B. Krogh-Jespersen, Y. Apeloig, M. Karni, J. Chandrasekhar, and P. V. R. Schleyer, *J. Am. Chem. Soc.*, **108**, 270 (1986).

14) S. Koda, *Chem. Phys. Lett.*, **55**, 353 (1978); S. Koda, *Chem. Phys.*, **66**, 383 (1982).

15) K. K. Murray, D. G. Leopold, T. M. Miller, and W. C. Lineberger, *J. Chem. Phys.*, **89**, 5442 (1988).

16) J. F. Harrison, R. C. Lieke, and J. F. Liebman, *J. Am. Chem. Soc.*, **101**, 7162 (1979); P. H. Muleer, N. G. Rondan, K. N. Houk, J. F. Harrison, D. Hooper, B. H. Willen, and J. F. Liebman, *J. Am. Chem. Soc.*, **103**, 5049 (1981).

17) J. Farras, S. Olivella, A. Sole, and J. Vilarrasa, *J. Comput. Chem.*, **7**, 428 (1986).

18) G. Frenking and W. Koch, *Chem. Phys. Lett.*, **138**, 503 (1987).

19) S. T. Gibson, P. J. Greene, and J. Berkowitz, *J. Chem. Phys.*, **83**, 4319 (1985).

20) C. F. Bender, J. H. Meadows, and H. F. Schaefer, III, *Faraday Discuss. Chem. Soc.*, **62**, 58 (1977).

21) S. D. Peyerimhoff and R. J. Buenker, *J. Chem. Phys.*, **42**, 167 (1979).

22) S. A. Pope, I. H. Hillier, and M. F. Guest, *Faraday Symp. Chem. Soc.*, **19**, 109 (1984).

23) J. A. Pople and P. V. R. Schleyer, *Chem. Phys. Lett.*, **129**, 279 (1986); J. A. Pople and I. A. Curtiss, *J. Phys. Chem.*, **91**, 155 (1987).

24) G. P. Ford and P. S. Herman, *J. Am. Chem. Soc.*, **111**, 3987 (1989).

25) K. A. Peterson, R. C. Mayrhofer, E. L. Sibert, III, and R. C. Woods, *J. Chem. Phys.*, **94**, 414 (1991).

26) M. O'Keeffe, *J. Am. Chem. Soc.*, **108**, 4341 (1986).

27) J. J. Fisher and T. B. McMahon, *J. Am. Chem. Soc.*, **110**, 7599 (1988).

28) J. F. Harrison and C. W. Eakers, *J. Am. Chem. Soc.*, **95**, 3467 (1973).

29) R. F. W. Bader, Y. Tal, S. G. Anderson, and T. T. Nguyen-Dang, *Isr. J. Chem.*, **19**, 8 (1980); R. F. W. Bader, T. T. Nguyen-Dang, and Y. Tal, *Rep. Prog. Phys.*, **44**, 893 (1981); R. F. W. Bader and T. T. Nguyen-Dang, *Adv. Quantum Chem.*, **14**, 63 (1981); R. F. W. Bader, "Atoms in Molecules. A Quantum Theory," Oxford Press, Oxford (1990).

30) W. R. Wadt and P. J. Hay, *J. Chem. Phys.*, **82**, 284 (1985).

31) C. Møller and M. S. Plesset, *Phys. Rev.*, **46**, 618 (1934); J. S. Binkley and J. A. Pople, *Int. J. Quantum Chem., Symp.*, **9S**, 229 (1975).

32) W. J. Hehre, R. Ditchfield, and J. A. Pople, *J. Chem. Phys.*, **56**, 2257 (1972).

33) A. Höllwarth, M Böhme, S. Dapprich, A. W. Ehlers, A. Gobbi, V. Jonas, K. F. Köhler, R. Stegmann, A. Veldkamp, and G. Frenking, *Chem. Phys. Lett.*, submitted.
34) J. A. Pople and R. K. Nesbet, *J. Chem. Phys.*, **22**, 571 (1954).
35) R. F. Hout, B. A. Levi, and W. J. Hehre, *J. Comput. Chem.*, **3**, 234 (1982); W. J. Hehre, L. Radom, P. v. R. Schleyer, and J. A. Pople, "Ab initio Molecular Orbital Theory," Wiley, New York (1986).
36) A. Gobbi and G. Frenking, unpublished.
37) R. Krishnan, J. S. Binkley, R. Seeger, and J. A. Pople, *J. Chem. Phys.*, **72**, 650 (1980); A. D. McLean and G. S. Chandler, *J. Chem. Phys.*, **72**, 5639 (1980).
38) "Gaussian 92, Revision A," M. J. Frisch, G. W. Trucks, M. Head-Gordon, P. M. W. Gill, M. W. Wong, J. B. Foresman, H. B. Schlegel, K. Raghavachari, M. A. Robb, J. S. Binkley, C. Gonzalez, R. Martin, D. J. Fox, D. J. DeFrees, J. Baker, J. J. P. Stewart, and J. A. Pople, Gaussian Inc., Pittsburgh, PA (1992).
39) F. W. Biegler-König, R. F. W. Bader, and T. Ting-Hua, *J. Comput. Chem.*, **3**, 317 (1982).
40) J. H. Meadows and H. F. Schaefer, III, *J. Am. Chem. Soc.*, **98**, 4383 (1986).
41) R. C. Ivery, P. D. Schultze, T. C. Leggett, and D. A. Kohl, *J. Chem. Phys.*, **60**, 3174 (1974).
42) M. Okumura, B. D. Rehfuss, B. M. Dinelli, M. G. Bawendi, and T. Oka, *J. Chem. Phys.*, **90**, 5918 (1989).
43) P. Jensen, P. R. Bunker, and A. D. McLean, *Chem. Phys. Lett.*, **141**, 53 (1987).
44) S. J. Dunlavey, J. M. Dyke, N. Jonathan, and A. Morris, *Mol. Phys.*, **39**, 1121 (1980).
45) A. B. Cornford, D. C. Frost, F. G. Herring, and C. A. McDowell, *J. Chem. Phys.*, **54**, 1872 (1971).
46) P. R. Bunker and P. Jensen, *J. Chem. Phys.*, **79**, 1224 (1983); P. Jensen, P. R. Bunker, and A. R. Hay, *J. Chem. Phys.*, **77**, 5370 (1982).
47) K. Fukui, *Acc. Chem. Res.*, **4**, 57 (1971); I. Fleming, "Frontier Orbitals and Organic Chemical Reactions," Wiley, New York (1976).
48) R. S. Mulliken, *Rev. Mod. Phys.*, **14**, 204 (1942); A. D. Walsh, *J. Chem. Soc.*, 2260 (1953); R. J. Buenker and S. D. Peyerimhoff, *Chem. Rev.*, **74**, 127 (1974); B. M. Gimarc, "Molecular Structure and Bonding: The Qualitative Molecular Orbital Approach," Academic Press, New York (1979).
49) P. J. MacDougall and R. F. W. Bader, *Can. J. Chem.*, **64**, 1496 (1986); C. Gatti, P. J. MacDougall, and R. F. W. Bader, *J. Chem. Phys.*, **88**, 3792 (1988).
50) The following values for the atomic radii were taken from Ref. 52: H, 0.30 Å; C, 0.77 Å; N, 0.70 Å; F, 0.64 Å; Cl, 0.99 Å; Br, 1.14 Å, I, 1.33 Å.
51) Page 196f in Ref. 29d.
52) L. Pauling, "The Nature of the Chemical Bond," Cornell University Press, (1960).
53) D. Cremer and E. Kraka, *Angew. Chem.*, **96**, 612 (1984); *Angew. Chem., Int. Ed. Engl.*, **23**, 627 (1984); G. Frenking, W. Koch, D. Cremer, J. Gauss, and J. F. Liebman, *J. Phys. Chem.*, **93**, 3410 (1989).
54) R. F. W. Bader, T. S. Slee, D. Cremer, and E. Kraka, *J. Am. Chem. Soc.*, **105**, 5061 (1983).
55) M. Fujitoka and E. Hirota, *J. Mol. Spectrosc.*, **97**, 491 (1973).
56) G. Herzberg and J. W. C. Johns, *Proc. R. Soc. London, Ser. A*, **295**, 107 (1960).
57) T. Noro and M. Yoshimine, *J. Chem. Phys.*, **91**, 3012 (1989).
58) T. Suzuki, S. Saito, and E. Hirota, *J. Mol. Spectrosc.*, **90**, 447 (1981).
59) M. Kakimoto, S. Saito, and E. Hirota, *J. Mol. Spectrosc.*, **97**, 194 (1983).
60) H. Petek, D. J. Nesbitt, P. R. Ogilby, and C. B. Moore, *J. Phys. Chem.*, **87**, 5367 (1983).
61) D. E. Milligan, D. E. Mann, M. E. Jacox, and R. A. Mitsch, *J. Chem. Phys.*, **41**, 1199 (1964); C. W. Mathews, *Can. J. Chem.*, **45**, 2355 (1967); A. S. Lefohn and G. C. Pimentel, *J. Chem. Phys.*, **55**, 1213 (1971); W. H. Kirchhoff, D. R. Lide, and F. X. Powell, *J. Mol. Spectrosc.*, **47**, 491 (1973); P. B. Davis, W. Lewis-Brown, and D. K. Russell, *J. Chem. Phys.*, **75**, 5602 (1981); P. B. Davies, P. A. Hamilton, J. M. Elliott, and M. J. Rice, *J. Mol. Spectrosc.*, **102**, 193 (1983); B. Burkholder, C. J. Howard, and P. A. Hamilton, *J. Mol. Spectrosc.*, **127**, 362 (1988).
62) D. E. Milligan and M. E. Jacox, *J. Chem. Phys.*, **48**, 2265 (1968).
63) D. E. Milligan and M. E. Jacox, *J. Chem. Phys.*, **47**, 703 (1967); L. Andrews, *J. Chem. Phys.*, **48**, 979 (1967).
64) M. E. Jacox and D. E. Milligan, *J. Chem. Phys.*, **53**, 2688 (1970).
65) D. E. Tevault and L. Andrews, *J. Mol. Spectrosc.*, **54**, 110 (1975).
66) L. Andrews and T. G. Carver, *J. Chem. Phys.*, **49**, 896 (1968).
67) D. E. Tevault and L. Andrews, *J. Am. Chem. Soc.*, **97**, 1707 (1975).
68) M. E. Jacox and D. E. Milligan, *J. Chem. Phys.*, **50**, 3252 (1969).
69) M. E. Jacox and D. E. Milligan, *J. Chem. Phys.*, **47**, 1626 (1967).
70) P. Jensen and P. R. Bunker, *J. Chem. Phys.*, **89**, 1327 (1988).